Title

CDK4-mediated MnSOD activation and mitochondrial homeostasis in radioadaptive protection

Authors

Jin, Cuihong
Qin, Lili
Shi, Yan
et al.

Publication Date

2015-04-01

DOI

10.1016/j.freeradbiomed.2014.12.026

Peer reviewed

Free Radical Biology and Medicine 81 (2015) 77–87

Contents lists available at ScienceDirect

Free Radical Biology and Medicine

journal homepage: www.elsevier.com/locate/freeradbiomed

Original Contribution

CDK4-mediated MnSOD activation and mitochondrial homeostasis in radioadaptive protection

Cuihong Jin [a,1,2], Lili Qin [a,1], Yan Shi [a], Demet Candas [a], Ming Fan [a], Chung-Ling Lu [a], Andrew T.M. Vaughan [a], Rulong Shen [b], Larry S. Wu [a], Rui Liu [a], Robert F. Li [a], Jeffrey S. Murley [c], Gayle Woloschak [d], David J. Grdina [c], Jian Jian Li [a,e,*]

[a] Department of Radiation Oncology, University of California at Davis School of Medicine, Sacramento, CA 95817, USA
[b] Department of Pathology, Ohio State University Medical College, Columbus, OH 43210, USA
[c] Department of Radiation and Cellular Oncology, University of Chicago, Chicago, IL 60637, USA
[d] Department of Radiation Oncology, Feinberg School of Medicine, Northwestern University, Chicago, IL 60611, USA
[e] NCI-Designated Comprehensive Cancer Center, University of California at Davis Health System, Sacramento, CA, 95817, USA

ARTICLE INFO

Article history:
Received 23 June 2014
Received in revised form
20 December 2014
Accepted 28 December 2014
Available online 8 January 2015

Keywords:
Cyclin D1/CDK4
Mitochondrial homeostasis
MnSOD
Phosphorylation
Radioadaptive response
Free radicals

ABSTRACT

Mammalian cells are able to sense environmental oxidative and genotoxic conditions such as the environmental low-dose ionizing radiation (LDIR) present naturally on the earth's surface. The stressed cells then can induce a so-called radioadaptive response with an enhanced cellular homeostasis and repair capacity against subsequent similar genotoxic conditions such as a high dose radiation. Manganese superoxide dismutase (MnSOD), a primary mitochondrial antioxidant in mammals, has long been known to play a crucial role in radioadaptive protection by detoxifying $O_2^{\bullet -}$ generated by mitochondrial oxidative phosphorylation. In contrast to the well-studied mechanisms of *SOD2* gene regulation, the mechanisms underlying posttranslational regulation of MnSOD for radioprotection remain to be defined. Herein, we demonstrate that cyclin D1/cyclin-dependent kinase 4 (CDK4) serves as the messenger to deliver the stress signal to mitochondria to boost mitochondrial homeostasis in human skin keratinocytes under LDIR-adaptive radioprotection. Cyclin D1/CDK4 relocates to mitochondria at the same time as MnSOD enzymatic activation peaks without significant changes in total MnSOD protein level. The mitochondrial-localized CDK4 directly phosphorylates MnSOD at serine-106 (S106), causing enhanced MnSOD enzymatic activity and mitochondrial respiration. Expression of mitochondria-targeted dominant negative CDK4 or the MnSOD-S106 mutant reverses LDIR-induced mitochondrial enhancement and adaptive protection. The CDK4-mediated MnSOD activation and mitochondrial metabolism boost are also detected in skin tissues of mice receiving in vivo whole-body LDIR. These results demonstrate a unique CDK4-mediated mitochondrial communication that allows cells to sense environmental genotoxic stress and boost mitochondrial homeostasis by enhancing phosphorylation and activation of MnSOD.

Low-level oxidative and genotoxic conditions such as low-dose ionizing radiation (LDIR) that is naturally present in the human living environment and in medical radiation use are potential cancer risks and have been public health concerns. Mammalian cells are able to generate an adaptive and homeostatic response to LDIR [1] with an enhanced ability to maintain genomic integrity and immunoresponsibility as well as to inhibit cell transformation [2–4]. Elucidation of the mechanisms underlying the LDIR-induced homeostatic response in mammalian cells will reveal new mechanistic insights into how cells coordinate with environmental toxic conditions, which will help in the invention of effective approaches to reduce and prevent environmental toxin-associated diseases.

Manganese superoxide dismutase (MnSOD) is a primary mitochondrial antioxidant enzyme in mammalian cells catalyzing the conversion of two molecules of superoxide anion ($O_2^{\bullet -}$) generated either as by-products of mitochondrial oxidative phosphorylation or under oxidative stress into hydrogen peroxide (H_2O_2), which is further oxidized to water [5,6]. In mouse epithelial skin cells, increased MnSOD activity is

* Corresponding author at: University of California Davis School of Medicine, Department of Radiation Oncology, 2700 Stockton Blvd, Sacramento, California 95817, United States. Fax: +916 734 4107.
E-mail address: jijli@ucdavis.edu (J.J. Li).
[1] These authors equally contributed to this study.
[2] Current address: Department of Toxicology, School of Public Health, China Medical University, 77 Puhe Road, Shenyang North New Area, Shenyang 110122, P.R. China.

http://dx.doi.org/10.1016/j.freeradbiomed.2014.12.026
0891-5849/

associated with LDIR-induced adaptive protection against subsequent lethal high-dose radiation [7]. In human mammary epithelial cells, LDIR induces MnSOD phosphorylation and enzymatic activation, which are required for the development of radioadaptive protection [8]. Increased MnSOD expression and enzymatic activity are linked to the radioadaptive response in either cultured cells or mice [9,10] and the MnSOD–NF-κB–MnSOD loop contributes to LDIR-induced radioprotection in brain and gut tissues from mice receiving whole-body LDIR [11]. In addition, MnSOD significantly reduces drug-induced cardiac injury by protecting mitochondria from damage caused by superoxide radicals [12] and protects normal esophageal, pancreatic, and bone marrow cells from radiation-induced genomic instability and apoptosis [13,14]. These findings suggest that the regulation of MnSOD expression and activation is implicated in the cellular genotoxic response. MnSOD is coded by the nuclear *SOD2* gene, and the NF-κB and tumor necrosis factor signaling pathways have been identified as important components in the regulation of *SOD2* expression [10,15]. The mitochondrial targeting sequence at the N terminus allows a direct transport of the newly synthesized MnSOD protein into the mitochondrion, where it self-associates into an active homotetramer containing Mn^{3+} ion and functions [16]. Recently, the posttranslational modification has been reported to play a pivotal role in the regulation of MnSOD enzymatic activation. For example, SIRT3-mediated deacetylation at multiple amino acid residues was found to elevate MnSOD antioxidant activity under oxidative stress in vitro and in vivo [17,18]. In LDIR-treated MCF10A cells, MnSOD is phosphorylated at serine-106 (S106), which stabilizes MnSOD protein, leading to increased enzymatic activity [8], whereas site-specific nitration at tyrosine-34 of MnSOD results in significant inactivation of its enzyme activity [19]. However, the mechanisms underlying the maintenance of mitochondrial homeostasis via posttranslational modification of MnSOD in the cellular adaptive response remain to be elucidated.

Cyclin D1 is involved in genotoxic stress through the regulation of mitochondrial function and cellular metabolism. In B cells, cyclin D1 inhibits mitochondria-mediated apoptosis induced by drug cytotoxic stress by altering the intracellular distribution of cell death regulators [20]. In LDIR-treated human skin keratinocytes, cytoplasmic cyclin D1 contributes to adaptive radioprotection by enhancing mitochondria-mediated antiapoptosis functions [21]. As the key regulator of the G1/S transition, in addition to regulating cell cycle progression [22], the cyclin D1/cyclin-dependent kinase 4 (CDK4) complex is involved in the regulation of mitochondrial function and cellular metabolism through a different subcellular localization [23–25]. Silencing CDK4 sensitizes cells to radiation-induced apoptosis by inhibiting phosphorylation of the apoptosis factor, which is independent of cell cycle progression [26]. In this study, we demonstrate that LDIR enhances mitochondrial homeostasis via mitochondrial-localized cyclin D1/CDK4 that directly phosphorylates MnSOD at Ser106, causing increased MnSOD activity and mitochondria respiration along with enhanced cell survival. These findings reveal a unique mechanism by which CDK4 communicates radiation stress to mitochondrial MnSOD, which allows the cell to adapt to the low level genotoxic stress via CDK4/MnSOD-controlled mitochondrial function and cell survival.

Materials and methods

Ethics statement

Female BALB/c mice age 6–8 weeks were irradiated with the indicated dose or dose combination following the protocol approved by the Institutional Animal Care and Use Committee of the University of California at Davis (IACUC No. 15315) and then dissected at the indicated times after radiation.

Antibodies and reagents

Rabbit polyclonal anti-cyclin D1, rabbit polyclonal anti-MnSOD, and mouse monoclonal anti-CDK4 antibodies were from Santa Cruz Biotechnology. Mouse monoclonal anti-α-tubulin, anti-β-actin, and anti-Flag antibodies were from Sigma. Mouse monoclonal anti-phosphoserine antibody was from Millipore. Rabbit polyclonal anti-cytochrome *c* oxidase subunit 4 (COX4) antibody was from Cell Signaling. Lipofectamine RNAiMAX and 2000 reagents, MitoSOX, and JC-1 were from Invitrogen. The QuikChange site-directed mutagenesis kit was from Agilent Technologies. Phosphatase inhibitor cocktail was from Sigma. The mitochondria isolation kit and protein A/G–Sepharose beads were from Pierce. The small interfering RNA (siRNA) construction kit was from Ambion.

Cells and treatment

Human skin keratinocytes (HK18) were cultured in Dulbecco's modified Eagle's medium supplemented with 10% fetal bovine serum and 1% penicillin/streptomycin (HyClone) in a humidified incubator (5% CO_2) and irradiated with a Faxitron Series cabinet X-ray system at a dose rate of 0.028 Gy/min (Hewlett Packard).

MnSOD activity assay

MnSOD activity assay was performed as described previously [27] with modifications. Briefly, cells were lysed in DETAPAC buffer (50 mM potassium phosphate buffer containing 1.34 mmol/L diethylenetriaminepentaacetic acid), sonicated with six 5- s bursts on ice, and centrifuged at 8000 *g* for 5 min at 4 °C. The assay reaction was initiated in DETAPAC buffer supplemented with 0.13 mg/ml bovine serum albumin, 1.25 U/ml catalase, 50 μM xanthine, 74.6 μM nitroblue tetrazolium (NBT), 50 μM bathocuproinedisulfonic acid with or without 5 mM NaCN by adding xanthine oxidase and incubated at room temperature for 2 min. The absorbance was monitored at 560 nm every 15 s for 2.5 min with the SpectraMax M2e plate reader (Molecular Devices). One unit of SOD activity was calculated as the amount of protein that inhibited NBT reduction by 50%.

Preparation of mitochondrial fractions from mouse tissues and cultured cells

Mitochondrial fractions were prepared using the published protocol [28] with modifications. Briefly, fresh mouse liver tissues were minced into small pieces and homogenized using a Teflon pestle in ice-cold IBc buffer (containing 0.2 M sucrose, 10 mM Tris/Mops, and 1 mM EGTA/Tris, pH 7.4) for 20 min, and the homogenates were centrifuged at 600 *g* for 10 min at 4 °C. The supernatant was collected and centrifuged at 7000 *g* for 10 min at 4 °C. The pellets were washed with ice-cold IBc buffer and resuspended in cell lysis buffer for either immediate use or storage at −80 °C for future use. Mitochondrial and cytosolic fractions of HK18 cells were obtained using a mitochondria isolation kit (Pierce) following the manufacturer's instructions.

Alkaline extraction

The alkaline extraction was performed as previously reported [29]. Briefly, the mitochondrial fraction was incubated in 0.1 M Na_2CO_3 (pH 11) for 20 min at 4 °C. The membrane was then pelleted by centrifugation at 100,000 *g*. Proteins in the supernatants were precipitated using a final volume of 10% trichloroacetic acid. The

pellets were resuspended in dissolving buffer containing 7 M urea, 3 M thiourea, 2% Chaps, 30 mM Tris, pH 8.5.

Cyclin D1/CDK4 kinase assay

For the in vitro CDK4 kinase assay, wild-type (wt) and mutant MnSOD were isolated from stably transfected cells by immunoprecipitation with anti-Flag antibody and incubated with 2 units of cyclin D1/CDK4 complex (New England Biolabs) in 30 μl of 1 × kinase assay buffer supplemented with 10 mM ATP and 100 μCi/μmol γ-^{32}P at 30 °C for 30 min. Samples were separated by SDS–PAGE followed by autoradiography.

Mitochondrial membrane potential (Δψm) assay

The Δψm was monitored using the JC-1 staining method (Invitrogen) following the manufacturer's instructions. Briefly, cells seeded in 96-well plates were incubated for 30 min at 37 °C in medium containing 2 μg/ml JC-1. After the cells were washed with phosphate-buffered saline (PBS; pH 7.4), the fluorescence intensity of JC-1 red and JC-1 green was detected using a SpectraMax M2e plate reader at excitation/emission wavelengths of 485 nm/595 nm and 485 nm/525 nm, respectively. The ratio of fluorescence intensity of JC-1 red to JC-1 green was used as an indicator of the Δψm.

Mitochondrial superoxide generation

Mitochondrial superoxide level was measured following the protocol published previously [27,30], with modifications. In brief, cells seeded in a 96-well plate were treated with the desired dose of radiation and washed with prewarmed 1 × PBS, pH 7.4, at indicated time points after radiation. One hundred microliters of 5 μM MitoSOX red working solution (diluted from a 5 mM stock solution in dimethyl sulfoxide with 1 × PBS, pH 7.4) was added to the cells and incubated for 10 min at 37 °C. The cells were washed twice with PBS and then the fluorescence intensity was detected directly in PBS using the SpectraMax M2e microplate reader at excitation/emission wavelengths of 510 nm/580 nm. The mitochondrial superoxide was shown as a percentage of the fluorescence generated in the control cells.

Oxygen consumption

Oxygen consumption was measured in HK18 cells or mitochondrial fractions isolated from fresh mouse tissues using a Clarke-type oxygen electrode (Rank Brothers) as described previously [28]. Exponentially growing cells were collected and 2 × 10^6 cells were resuspended in 300 μl oxygen consumption buffer containing 25 mM sucrose, 15 mM KCl, 1 mM EGTA, 0.5 mM $MgCl_2$, and 30 mM K_2HPO_4. Oxygen consumption was monitored at 30 °C with succinate as the complex II substrate. For the oxygen consumption of mouse liver, mitochondrial fractions in oxygen consumption buffer at a final concentration of 1 mg/ml were used.

Mitochondrial ATP production

Mitochondrial ATP production was tested using a published method [31] with modifications. In brief, cells seeded in a 96-well plate were permeabilized by adding digitonin (25 μg/ml) and shaken on ice for 1 min. Thirty microliters of buffer containing *P*1, *P*5-di(adenosine pentaphosphate) (0.15 mM), ADP (0.1 mM), malate (1 mM), and pyruvate (1 mM) with and without oligomycin (1 μg/ml) was added to the cells and incubated at room temperature for 5 min. Trichloroacetic acid (2.5%) was then added to the cells and ATP extracts were neutralized by adding Tris–acetate (pH 7.75) buffer and monitored using an ATP determination kit (Invitrogen).

Apoptosis assay

HK18 cells with the desired dose of irradiation or no-radiation shams were collected and resuspended in 500 μl of annexin-binding buffer (Biosource, Invitrogen) at 2 × 10^6 cells/ml. Cells were stained by adding 1 μl of FITC-conjugated annexin V (Biosource, Invitrogen) and propidium iodide (Sigma) to 100 μl of cell suspension followed by incubation at room temperature for 15 min in the dark. Each sample was then filled with 400 μl of annexin-binding buffer and the percentage of apoptotic cells was determined using flow cytometry immediately by counting 10,000 cells per sample.

Clonogenic survival assay

Cells treated with the desired dose or dose combinations were plated in 60-mm plates at various cell numbers and cultured for 10 days. The colonies formed were then stained with crystal violet and the numbers of colonies (with more than 50 cells) were counted, and the clonogenic survival ability of the irradiated cells was represented as the survival fraction after being normalized to the controls.

Plasmid constructs and cell transfection

For mitochondria-targeted gene expression, a mitochondria-targeting sequence (MTS) derived from the precursor of human cytochrome *c* oxidase subunit 8 A (COX8) was cloned into the pEGFP-N1 and pERFP-N1 vectors (Clontech) at the NheI and BamHI sites. Cyclin D1 or CDK4 cDNA was then cloned into pEGFP-N1-COX8 or pERFP-N1-COX8 plasmid at the BamHI site in frame with the COX8 sequence. MnSOD cDNA was cloned into the pcDNA3.1-flag vector (Invitrogen) at the EcoRI and XhoI sites. CDK4 D158N dominant negative and MnSOD S106A inactive mutants were generated using the QuikChange site-directed mutagenesis kit. The primer sequences for all plasmid constructs are listed in Supplementary Table S1. Exponentially growing HK18 cells were transfected using Lipofectamine 2000 and the stable transfectants were selected with G418 (500 μg/ml).

Cyclin D1 silencing by siRNA

SiRNA targeting cyclin D1 mRNA was synthesized with the Silencer siRNA construction kit (Ambion, Austin, TX, USA). Cells were seeded in 35-mm plates to achieve 30–50% confluence and cultured for 24 h before transfection was performed using Lipofectamine RNAiMAX reagent (Invitrogen, Carlsbad, CA, USA). Scramble RNA Duplex (Ambion) was included as control. Inhibition of cyclin D1 expression was determined by Western blotting at 24 h posttransfection. The primers used to synthesize the siRNA are listed in Supplementary Table S2.

Immunoblot (IB) and immunoprecipitation (IP)

For immunoblot, 20 μg of total cell lysates and cytosolic and mitochondrial fractions were separated by SDS–PAGE and transferred to a polyvinylidene difluoride membrane followed by immunoblotting with antibodies specific to the proteins of interest. The purity of the fractions was verified by immunoblot with COX4 and α-tubulin as markers of mitochondria and cytosol protein, respectively.

For co-IP/IB analysis, total and mitochondrial proteins (200 μg) were precleaned with normal mouse or rabbit IgG

and 20 μl of a 1:1 slurry of protein A/G–Sepharose beads for 1 h at 4 °C. Precleaned samples were immunoprecipitated with antibodies against proteins of interest overnight at 4 °C, followed by 3 h incubation with protein A/G beads. Beads were then collected by a brief spin down, washed three times with ice-cold 1 × PBS, and boiled in SDS–PAGE gel loading buffer. Samples were then fractionated by SDS–PAGE followed by immunoblot with the desired antibodies. Immunoprecipitation with normal rabbit or mouse IgG was used as a negative control.

Immunohistochemistry

The dorsal skin tissues from female BALB/c mice either untreated or irradiated were embedded, frozen, and sliced into tissue sections. For hematoxylin and eosin (H&E) staining, the tissue sections were deparaffinized in xylene 3 × 5 min and rehydrated in 100, 95, 85, and 75% ethanol for 5 min each, followed by rinsing with tap water for 5 min. Sections were stained with hematoxylin for 5 min at room temperature and rinsed with deionized H_2O. The sections were rinsed with running tap water for 5 min and dunked in acid alcohol (1% HCl in 70% EtOH) until the sections turned pink. The sections were washed with running tap water for 5 min and stained with eosin for 5 min followed by dehydration with 95% ethanol for 3 × 5 min and 100% ethanol for 3 × 5 min. The sections were soaked in xylene for 3 × 15 min to clean the water. The sections were then ready for imaging. Radiation-induced skin tissue injury was scored by people blinded to the treatment of each sample.

Statistical analysis

SPSS13.0 software was used to analyze the data. The variances are presented as the mean ± SEM. Statistical significance among groups was determined by using the two-tailed Student *t* test or ANOVA along with a post hoc Student Newman–Keul test. The data were considered significant at $P < 0.05$.

Results

Low-dose ionizing radiation induces adaptive protection in immortalized human skin keratinocytes

To investigate the mechanisms by which mammalian cells respond to low levels of genotoxic stress, we first tested the response of cells to 5 Gy irradiation with/without 10 cGy low-dose irradiation pretreatment using HK18 cells as an in vitro model system. We found that the apoptosis rate of the cells caused by 5 Gy lethal high-dose irradiation was significantly reduced by 10 cGy low-dose irradiation pretreatment (Fig. 1A), which was paralleled by a lowered mitochondrial $O_2^{\bullet -}$ (Fig. 1B). This result is consistent with our previous findings showing that 10 cGy pretreatment increases the clonogenic survival ability in HK18 cells exposed to a following challenging dose of 5 Gy radiation compared to cells exposed to 5 Gy radiation alone [21], confirming that LDIR is indeed a reliable stress source to induce the adaptive response in mammalian cells. Furthermore, MnSOD activity was increased in cells exposed to 10 cGy + 5 Gy IR compared to cells treated with 5 Gy alone (Fig. 1C), indicating that LDIR-induced adaptive protection might be mediated by MnSOD enzymatic activation.

Enhanced MnSOD activity and mitochondrial metabolism in LDIR-induced adaptive response

Next, we tested the response of HK18 cells to 10 cGy LDIR. The mitochondrial membrane potential was dramatically enhanced in the HK18 cells in response to LDIR, with a peak at 6 h after radiation (Fig. 2A). MnSOD activity was induced, also peaking at 6 h after radiation with a 36% increase compared to the sham no-radiation control (Fig. 2B); however, the total cellular MnSOD and mitochondrial MnSOD did not show a significant increase (Fig. 2C).

Because the MnSOD protein level did not correlate with the increased MnSOD enzymatic activity in these cells, we were wondering if the enhanced MnSOD activity could be linked to the potential posttranslational modification. Indeed, co-IP analysis detected a substantial amount of serine-phosphorylated MnSOD in LDIR-treated HK18 cells (Fig. 2F), which, together with our previous observation of CDK1-mediated MnSOD activation [8], suggests the serine-phosphorylated MnSOD is required for enhancing MnSOD enzymatic activity and mitochondrial homeostasis in LDIR-induced adaptive protection. The cellular oxygen consumption (Fig. 2D) and mitochondrial ATP generation (Fig. 2E) also peaked at 6 h, indicating that posttranslational modification of MnSOD is linked with LDIR-induced mitochondrial homeostasis.

Cyclin D1/CDK4 translocates to mitochondria and phosphorylates MnSOD

We then sought the kinase mediating LDIR-induced MnSOD serine phosphorylation. Although cyclin D1 is shown to regulate mitochondrial function [24] and MnSOD activity [32], the exact mechanism of cyclin D1-controlled MnSOD activity is unknown. Here, we found that a substantial amount of cyclin D1 and CDK4 was localized in mitochondria in HK18 cells after LDIR with a peak accumulation similar to MnSOD enzymatic activation without evident increase in cytosolic fractions (Fig. 3A and B). The total cellular cyclin D1 and CDK4 levels were significantly enhanced (Supplementary Fig. S1), indicating that most of the LDIR-induced cyclin D1/CDK4 proteins are

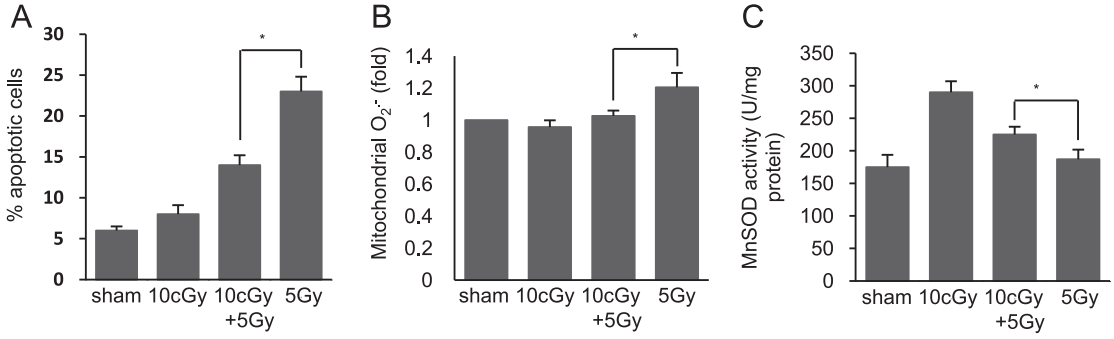

Fig. 1. Enhanced MnSOD enzymatic activity in LDIR-induced adaptive radioprotection in human skin keratinocytes. Human skin keratinocyte HK18 cells exposed to various doses or dose combinations of radiation (sham, 10 cGy, 10 cGy + 5 Gy, and 5 Gy) were collected at the desired time points for measuring (A) apoptosis, (B) mitochondrial superoxide level, and (C) MnSOD enzymatic activity. Means ± SEM; $^*P < 0.05$; $n \geq 3$.

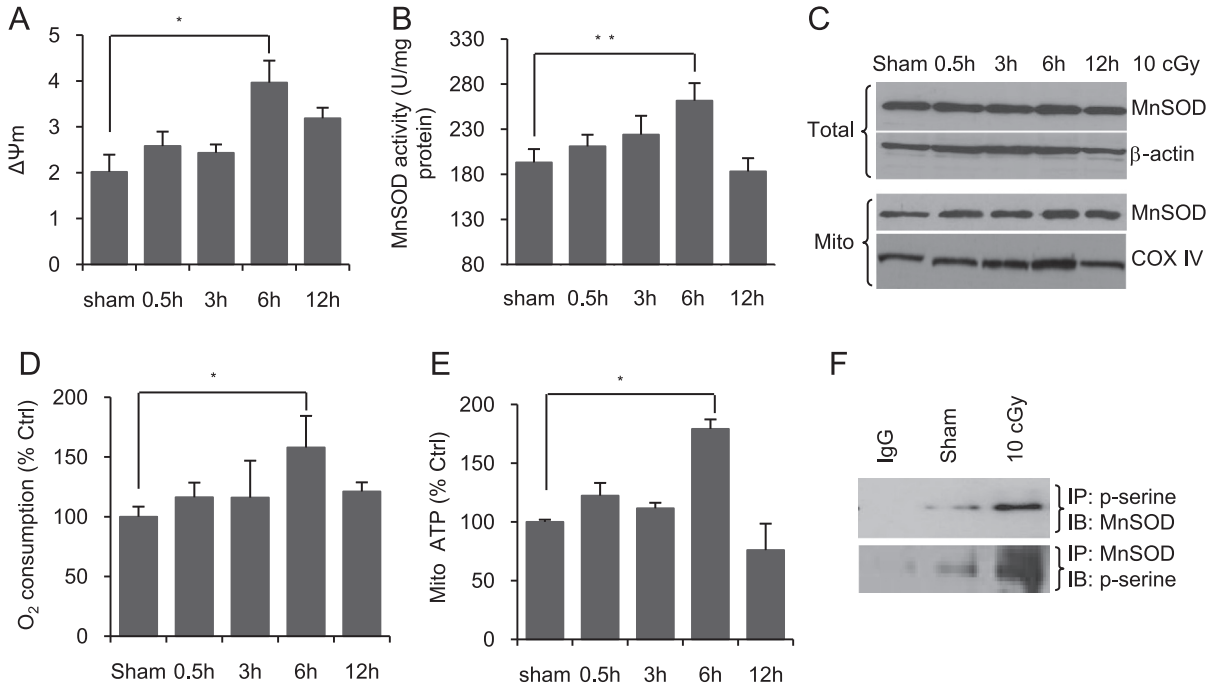

Fig. 2. MnSOD posttranslational modification is involved in LDIR-induced adaptive radioprotection. (A–E) HK18 cells were exposed to 10 cGy irradiation and collected at indicated times for measuring (A) mitochondrial membrane potential, (B) MnSOD activity, (C) MnSOD protein levels in total cell lysate and mitochondrial fractions by Western blot, (D) oxygen consumption, and (E) mitochondrial ATP generation. Sham, nonirradiated control. Means ± SEM; $^{*}P < 0.05$; $^{**}P < 0.01$; $n \geq 3$. (F) Enhanced MnSOD serine phosphorylation in LDIR-treated HK18 cells detected by co-IP with anti-p-serine followed by IB with anti-MnSOD and vice versa.

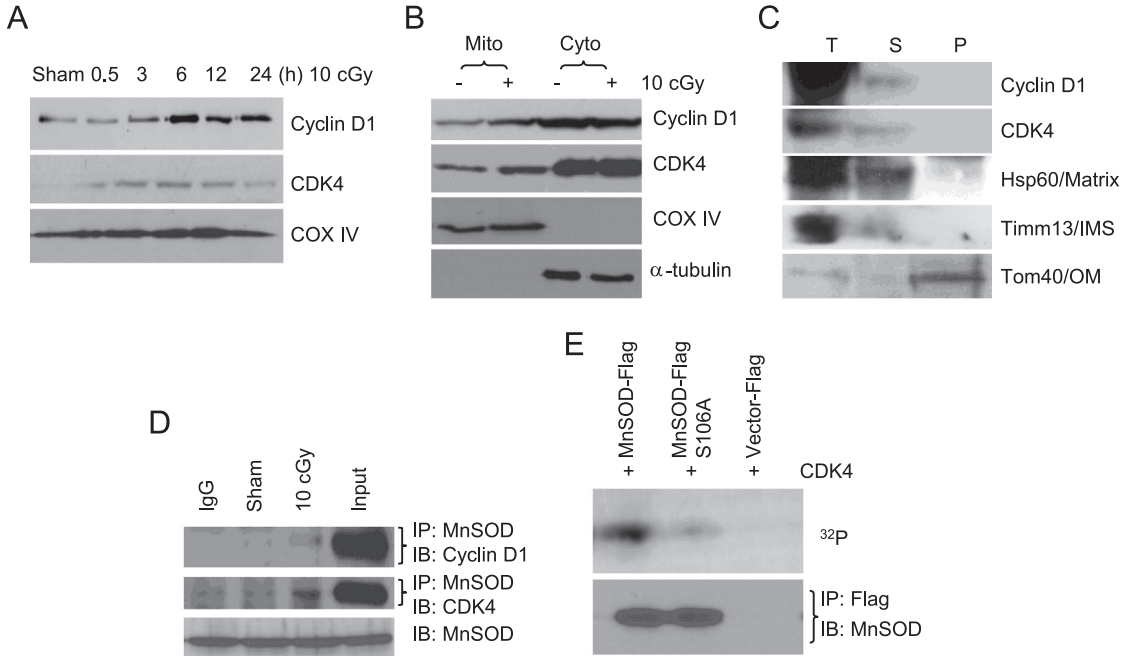

Fig. 3. Cyclin D1/CDK4 relocates into mitochondria in response to LDIR. (A) LDIR induces mitochondrial translocation of cyclin D1 and CDK4 in HK18 cells. (B) Mitochondrial but not cytosolic cyclin D1/CDK4 complex was increased in response to LDIR. COX4 and α-tubulin were used to confirm the purity of mitochondrial and cytosol fractions, respectively. (C) Identification of submitochondrial localization of cyclin D1/CDK4. T, total mitochondrial fraction; S, soluble matrix and intermembrane proteins; P, membrane pellets. IMS, intermembrane space; OM, outer membrane. Hsp60, Timm13, and Tom40 serve as markers of mitochondrial matrix, intermembrane space, and outer membrane, respectively. (D) LDIR enhances protein interaction between MnSOD and cyclin D1/CDK4 complex in mitochondria. MnSOD without IP serves as the equal input control. (E) Cyclin D1/CDK4 complex phosphorylates MnSOD on S106. Immunoblots of immunoprecipitation reactions with MnSOD antibody were used to confirm the equal amounts of MnSOD used for each kinase assay reaction.

localized in the mitochondria. Alkaline extraction analysis revealed that cyclin D1 and CDK4 were localized in the mitochondrial matrix and/or intermembrane space in mitochondria, but not on the outer or inner membrane (Fig. 3C). Furthermore, coimmunoprecipitation assays showed an increased cyclin D1/CDK4/MnSOD interaction in cells collected at 6 h after 10 cGy irradiation (Fig. 3D), which together with results of the in vitro CDK4 kinase assay using either wild-type or S106A mutant MnSOD (Fig. 3E), suggests that cyclin D1/CDK4

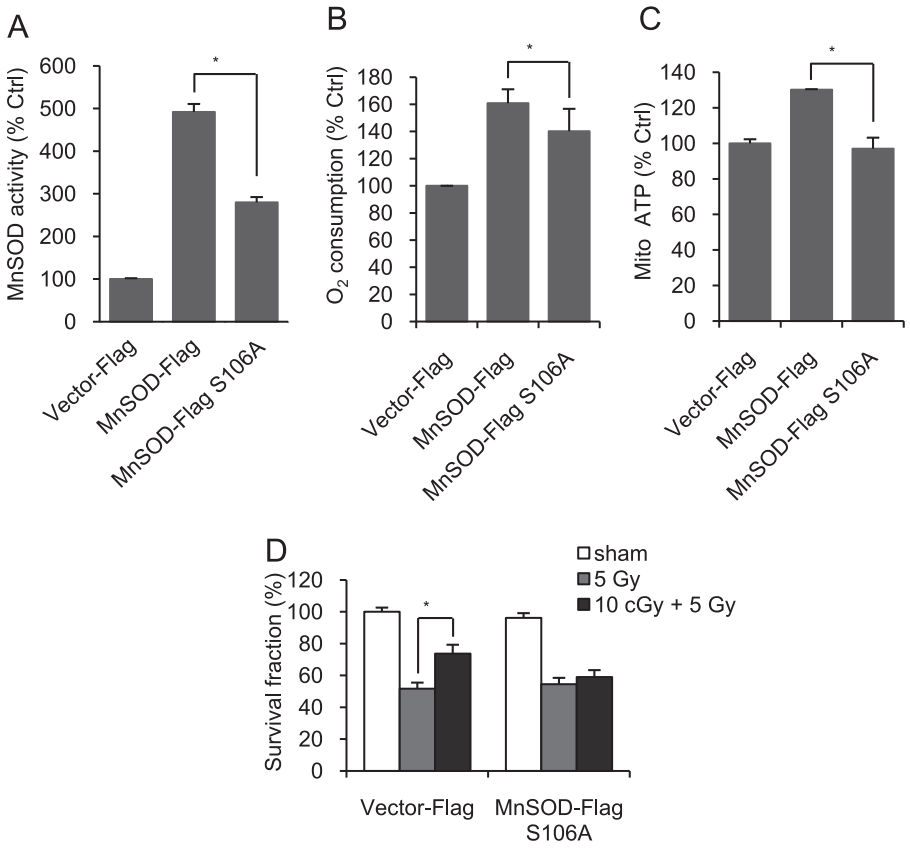

Fig. 4. Serine-106 phosphorylation is required for MnSOD activation and LDIR-induced mitochondrial respiration. HK18 cells were transfected with either wild-type or S106A-mutant MnSOD and stably transfected cells were collected at 6 h after LDIR for measuring (A) MnSOD activity, (B) oxygen consumption, (C) mitochondrial ATP generation, and (D) clonogenic survival assay. Means ± SEM; $^{*}P < 0.05$; $n \geq 3$.

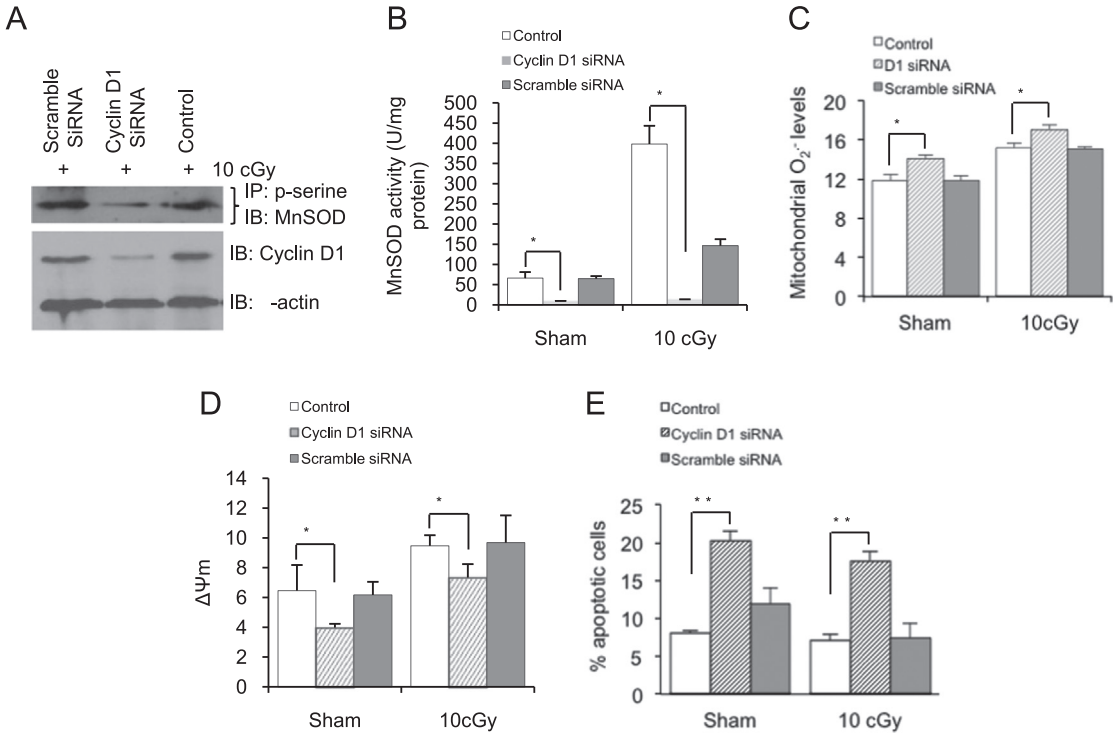

Fig. 5. Cyclin D1 is required for MnSOD activation and enhanced mitochondrial respiration in LDIR-induced radioprotection. HK18 cells were transfected with cyclin D1-specific siRNA, scrambled siRNA, or reagents only and irradiated with 10 cGy 48 h after transfection. At 6 h after radiation, the cells were collected to measure (A) p-serine MnSOD, (B) MnSOD activity, (C) mitochondrial superoxide, (D) mitochondrial membrane potential, and (E) apoptosis. Control, no siRNA transfection. Means ± SEM; $^{*}P < 0.05$, $^{**}P < 0.01$; $n \geq 3$.

directly phosphorylates MnSOD at S106, a minimal motif of serine/threonine kinase substrate.

Serine-106 phosphorylation is required for enhanced MnSOD activity and mitochondrial respiration in adaptive radioprotection in HK18 cells

To confirm if S106 phosphorylation is required for MnSOD activation and enhanced mitochondrial metabolism, we constructed wild-type and S106A mutant MnSOD-expressing plasmids and established stable transfectants in HK18 cells. Plasmid constructs and confirmation of stable transfectants are shown in Supplementary Figs. S2A and S2B. We found that MnSOD activity was enhanced in wt but not S106A mutant MnSOD transfectants (Fig. 4 A) and a substantial amount of LDIR-enhanced oxygen consumption and mitochondrial ATP generation was lost in the S106A mutant MnSOD transfectants (Fig. 4B and C), indicating that MnSOD S106 phosphorylation is required for its enzymatic activation and mitochondrial oxidative respiration. In addition, 10 cGy pretreatment of S106A mutant MnSOD-transfected HK18 cells did not show significant protection from the following 5 Gy radiation compared to empty vector control cells tested by clonogenic survival assay (Fig. 4D), suggesting that S106 phosphorylation contributes to the MnSOD-mediated cell adaptive response and might be the only phosphorylation event that functions in this radioadaptive response, supporting that S106 phosphorylation of MnSOD is required by the LDIR-induced adaptive response.

Cyclin D1 is required for MnSOD activation in LDIR-induced radioprotection

To determine whether cyclin D1 is required for MnSOD activation and LDIR-induced adaptive protection, we performed siRNA-mediated knockdown in HK18 cells. We found that cyclin D1 siRNA-transfected cells had a lower level of LDIR-induced p-serine MnSOD (Fig. 5A) and MnSOD activity (Fig. 5B), along with increased mitochondrial superoxide (Fig. 5C), reduced $\Delta\psi m$ (Fig. 5D), and increased apoptosis (Fig. 5E) compared to scrambled siRNA and transfection-reagent-only control cells. Combined with our published data showing that HK18 cells treated with cyclin D1 siRNA are deficient in LDIR-induced clonogenic radioprotection ability compared to scrambled siRNA-treated control cells [21], these results suggest that cyclin D1 is required for MnSOD activation and adaptive response in HK18 cells.

The CDK4 kinase domain is required in LDIR-induced adaptive protection

To further confirm the role of cyclin D1/CDK4-mediated MnSOD S106 phosphorylation in MnSOD activation and adaptive radioprotection in HK18 cells, we constructed mitochondria-targeted cyclin D1 and CDK4 (either wild type or D158N kinase domain dominant negative mutant)-expressing plasmids (Supplementary Fig. S3A). Mitochondrial localization of MTS-cyclin D1 and MTS-CDK4-wt in the stable transfectants was verified by fluorescence microscopy

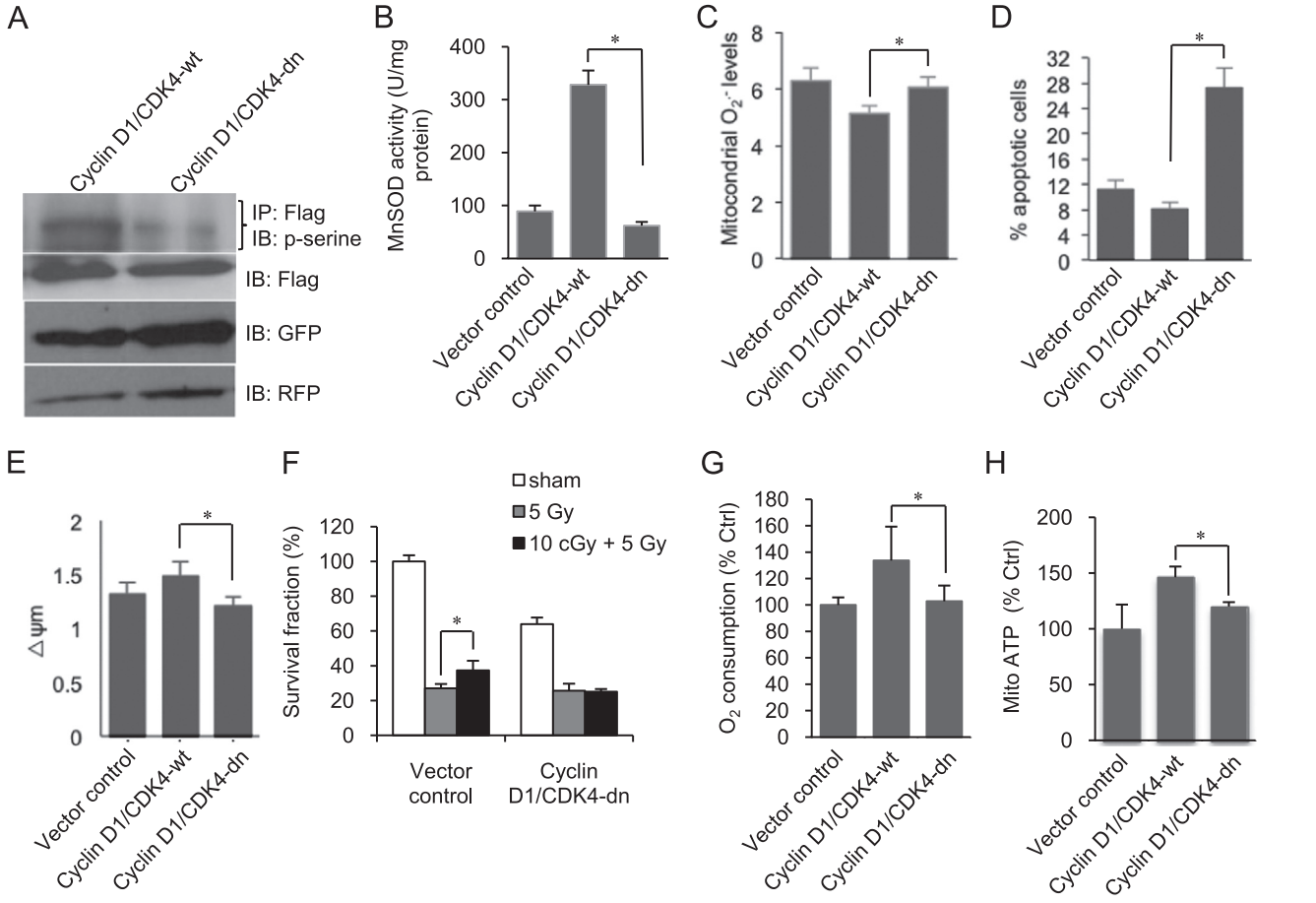

Fig. 6. CDK4 kinase activity is required for enhanced mitochondrial respiration and mitochondria-mediated antiapoptosis. (A) HK18 cells were cotransfected with MTS-CDK4-wt or MTS-CDK4-dn along with cyclin D1, and p-serine MnSOD levels were measured at 6 h after radiation in stable transfectants further transfected with MnSOD-Flag. (B–H) HK18 cells cotransfected with MTS-CDK4-wt or MTS-CDK4-dn along with cyclin D1 were treated with 10 cGy radiation and collected at 6 h after radiation to measure (B) MnSOD activity, (C) mitochondrial superoxide, (D) apoptosis, (E) mitochondrial membrane potential, (F) clonogenic survival, (G) oxygen consumption, and (H) mitochondrial ATP production. MTS, mitochondria-targeting sequence; wt, wild-type CDK4; dn, D158N dominant negative mutant. GFP (green fluorescent protein) and RFP (red fluorescent protein) were used to confirm equal amounts of inputs. Means ± SEM; $^{*}P < 0.05$; $n \geq 3$.

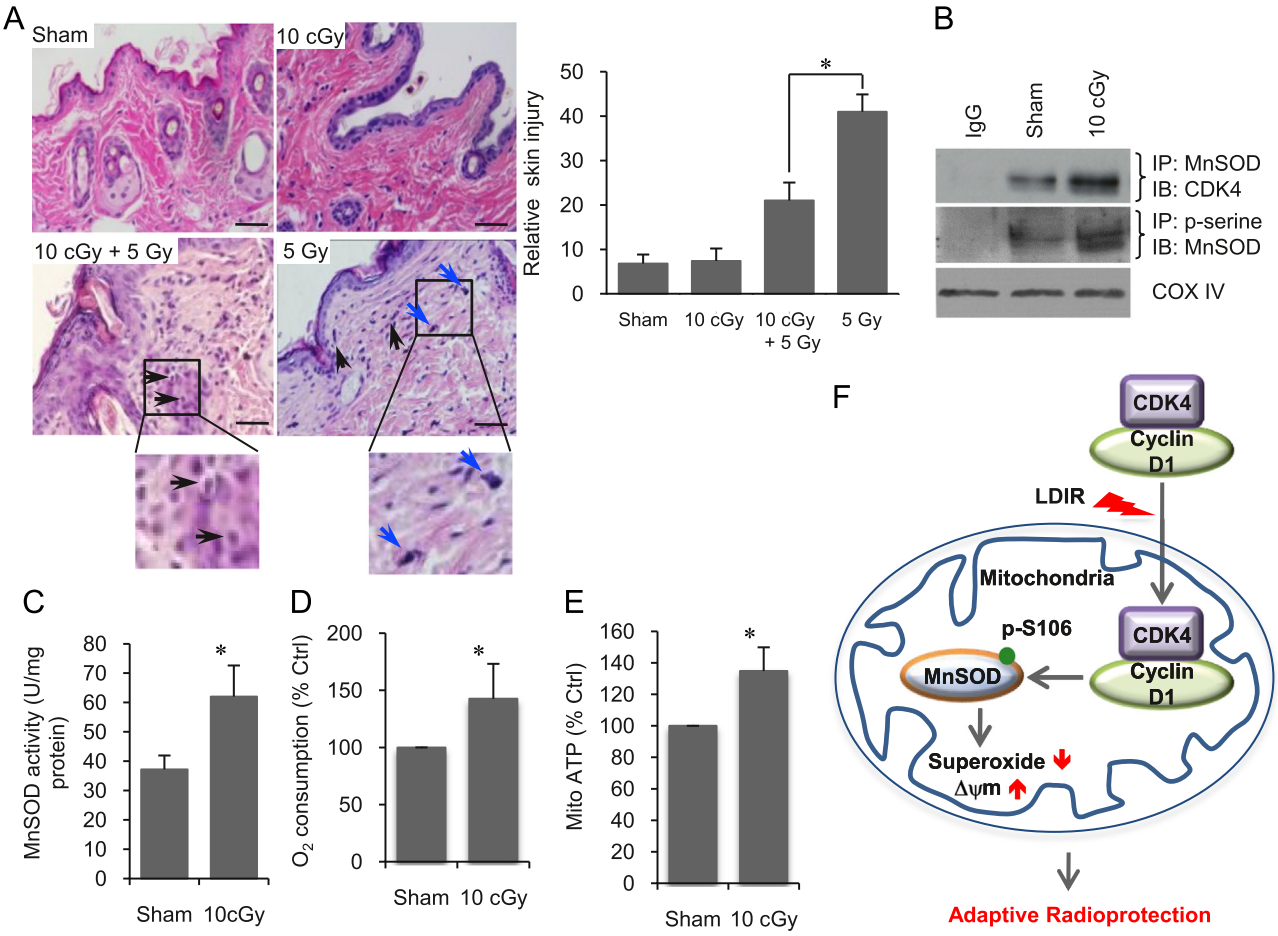

Fig. 7. The cyclin D1/CDK4/MnSOD pathway in LDIR-induced adaptive protection in vivo. Female BALB/c mice were exposed to whole-body irradiation with various dose combinations (sham, 10 cGy, 5 Gy, or 10 cGy+5 Gy) or a single low dose (10 cGy). The mice were then dissected at the desired time points after irradiation and tissues were used for immunohistochemistry assay or preparation of mitochondrial fractions. Means ± SEM; $^{*}P<0.05$; $n\geq 3$. (A) Representative histological changes and quantitative results of inflammatory cells in skin epidermal tissues from mice that received the indicated doses of whole-body irradiation. Mice were exposed to 10 cGy, 10 cGy+5 Gy, or 5 Gy irradiation and dissected at the desired time points after radiation. Mouse skin tissues were embedded and sliced. The tissue sections were subjected to H&E staining and the images are presented to show the skin injury by irradiation. Black arrows, lymphocyte infiltration. Blue arrows (5 Gy), abundant fibroblast proliferation. Sham, no-radiation control. Scale bar, 50 μm. (B) Enhanced CDK4 interaction with MnSOD and increased MnSOD phosphorylation in mitochondria of skin epidermal layers from 10 cGy-irradiated mice. (C) MnSOD activity measured in skin epidermal tissues from mice treated with 10 cGy irradiation. (D) Enhanced mitochondrial oxygen consumption in livers from 10 cGy-irradiated mice. (E) Enhanced mitochondrial ATP production in livers from 10 cGy-irradiated mice. (F) Schematic of the CDK4/MnSOD signaling pathway in LDIR-induced cellular adaptive protection. LDIR induces cyclin D1/CDK4 mitochondrial relocation and phosphorylation of MnSOD at serine-106, causing an enhanced mitochondrial homeostasis via MnSOD activation and oxidative respiration.

(Supplementary Fig. S3B). The stably transfected cells were treated with 10 cGy low-dose radiation and collected at 6 h after radiation for each experiment. Consistent with the higher level of p-serine MnSOD (Fig. 6A), MnSOD activity was remarkably enhanced (approx seven-fold; Fig. 6B), along with decreased mitochondrial $O_2^{\bullet-}$ (Fig. 6C), in the MTS-CDK4-wt cells but not the MTS-CDK4-dn cells compared to empty vector control cells. Contrasted with MTS-CDK4-dn cells, MTS-CDK4-wt cells showed reduced apoptosis (Fig. 6D) and increased mitochondrial membrane potential (Fig. 6E). To further confirm CDK4-mediated adaptive resistance, we did the clonogenic survival assay and found that the colony formation ability of MTS-CDK4-dn cells receiving 5 Gy radiation was not significantly increased by 10 cGy pretreatment (Fig. 6F). Compared with wild-type CDK4, the oxygen consumption (Fig. 6G) and mitochondrial ATP generation (Fig. 6H) were decreased in the MTS-CDK4-dn cells.

Cyclin D1/CDK4/MnSOD pathway in LDIR-induced adaptive protection in vivo

Wondering if the cyclin D1/CDK4/MnSOD pathway causes LDIR-induced adaptive response in vivo, we treated BALB/c mice with whole-body radiation with the established regimen of radiation dose or dose combination (sham, 10 cGy, 10 cGy+5 Gy, 5 Gy) and dissected the mice at the desired time points after radiation. Samples of whole skin tissues were extracted, fixed, embedded, and sliced for H&E staining. Radiation-induced skin injury was analyzed using the following criteria: (1) the layers of the skin, especially dermis, become thinner; (2) the regular histological structure of the skin is destroyed; (3) the cells undergo apoptosis or necrosis; and (4) in some cases, inflammatory cells that infiltrated the dermis layer were counted. As is shown in Fig. 7A, we found that the mice receiving LDIR pretreatment showed less radiation injury to skin, with reduction of inflammatory cells and fibroblast proliferation, after exposure to a challenging single high dose of radiation. In the skin epidermal tissues isolated from mice exposed to whole-body LDIR, MnSOD activity was increased ~40% (Fig. 7C), which paralleled an enhanced CDK4/MnSOD interaction and increased level of p-serine MnSOD (Fig. 7B). Consistent with the features of mitochondrial respiration in irradiated cultured cells, mitochondrial oxygen consumption and ATP production were increased in the mitochondrial fractions isolated from liver tissues (Fig. 7D and E) of LDIR-treated mice.

Discussion

Mitochondrial homeostasis is believed to play a key role in the stress-induced adaptive response. In this study, we demonstrated for the first time that the cyclin D1/CDK4 complex can relocate to mitochondria in the radiation-induced adaptive response, contributing to mitochondrial homeostasis via MnSOD phosphorylation and enzymatic activation. The CDK4-mediated posttranslational modification of MnSOD may serve as a critical pathway for the quick enhancement of mitochondrial metabolism for ATP generation and cell survival. CDK4 is a critical cell cycle regulator controlling the G1/S transition [33], and in glucose metabolism and insulin secretion, it regulates the associated gene expression [34]. Nuclear cyclin D1 accompanied by its kinase partner CDK4 induces cell cycle progression, but in postmitotic cells cyclin D1 is mainly localized in the cytoplasm [35]. Although the cytoplasmic sequestration of cyclin D1 is required for the survival of postmitotic neurons, and nuclear relocalization of cyclin D1 induces apoptosis [25], there is no direct evidence for CDK4-mediated mitochondrial targets. However, cytosolic accumulation of cyclin D1 is required to enhance antiapoptosis with improved mitochondrial membrane potential [21]. The current study reveals that a fraction of CDK4 is physically localized in the mitochondria. The mitochondrial cyclin D1/CDK4 complex is able to reduce mitochondrial superoxide levels via phosphorylation (S106) and activation of MnSOD and by boosting the overall mitochondrial bioenergetics. A cluster of mitochondrial respiratory chain complex I subunits has just been identified to be substrates of cyclin B1/CDK1 for enhancing mitochondrial ATP generation required for cell cycle G2/M progression [36]. The exact mechanism underlying CDK4/MnSOD activation-mediated mitochondrial homeostasis and ATP generation is to be further investigated.

Contrasted with well-studied aspects of MnSOD, including gene transcription and protein folding, potential MnSOD posttranslational modifications and their physiologic functions are not well understood. $O_2^{\bullet -}$ is generated as the by-product of mitochondrial oxidative respiration as well as by different forms of oxidative stress including ionizing radiation; both can cause primary damage in mtDNA and other mitochondrial macromolecules [37]. Mitochondrial $O_2^{\bullet -}$ is the major source of cellular reactive oxygen species (ROS), which are considered to function as redox signaling molecules [38] and may serve as a sensor for genotoxic stress and aging [39,40]. MnSOD is encoded by genomic DNA but its antioxidant ability is fully activated after mitochondria translocation through a set of posttranslational modifications, including acetylation/deacetylation, phosphorylation/dephosphorylation, and nitration [41]. The current study using in vitro-irradiated human skin keratinocytes and in vivo-irradiated mouse tissues demonstrates that cyclin D1/CDK4-mediated phosphorylation of mitochondrial MnSOD is required for the elevated antioxidant ability of MnSOD, which compensates for the increased cytotoxic ROS due to enhanced mitochondrial respiration. How phosphorylation of MnSOD affects its enzyme activity is still not clear. Our recent study showed that cyclin B1/CDK1 links the cell cycle G2/M transition via CDK1-mediated phosphorylation and activation of the mitochondrial respiration chain [36] and CDK1 also phosphorylates MnSOD at the same site, S106, which stabilizes MnSOD protein and enzymatically activates MnSOD possibly in the LDIR-induced adaptive response [8]. Although the exact mechanism of phosphorylation-mediated MnSOD enzymatic activation remains to be solved, the negative charges introduced by phosphorylation might enhance the affinity of the SOD2 protein to the Mn^{2+} ion whose incorporation into the protein is necessary for SOD2 enzymatic activation during its mitochondrial translocation. In addition, S106 phosphorylation may enhance and stabilize MnSOD homotetramer conformation, which has been proven to contribute to the enzyme stability and activity of human mitochondrial MnSOD [16]. Our current data also suggest that the posttranslational modifications of MnSOD proteins may be able to induce a quick adaptive reaction without the need of substantial regulation of *SOD2* gene transcription in response to genotoxic stresses. We have previously observed that in the LDIR-induced adaptive response of mouse skin epithelial cells, the MnSOD protein level is significantly induced by either single LDIR or fractionated LDIR compared to no-radiation control, paralleled by enhanced enzyme activity [7]. In human skin keratinocytes, however, in the present studies, MnSOD enzymatic activity was significantly enhanced without a detectable increase in the protein level, indicating that different mechanisms might be involved in mouse and human cells for mitochondrial antioxidant regulation. Interestingly, MnSOD phosphorylation on the serine/threonine site is reported to decrease its enzyme activity in plant and bacteria [41], leaving the specific phosphorylation site unidentified, indicating that phosphorylation of MnSOD at different amino acids might lead to different effects on its enzyme activity. Thus, it is highly possible that different mechanisms are adopted by various species to enhance mitochondrial antioxidants and homeostasis under genotoxic stress conditions. The mechanisms underlying cell cycle regulator (CDK1 and CDK4)-mediated MnSOD S106 phosphorylation and enzymatic activation in LDIR-induced adaptive response and mitochondrial homeostasis need to be further investigated.

As is shown in our model in Fig. 7F, MnSOD activity is induced by preexposure of 10 cGy radiation, which is in agreement with our previously reported results [7,8], leading to the increased mitochondrial homeostasis. Increased mitochondrial superoxide is reported to contribute to the release of redox-active metal ions, such as Fe(II) and Cu(I), which can be deleterious to cells because of the generation of highly reactive hydroxyl radical $^{\bullet}OH$ and OH^- by the Fenton reaction [42,43], and multiple human diseases including cancer and neuronal diseases [44–46]. We did not test these redox-active metal ions in this study, but it is highly possible that LDIR-induced MnSOD activation protects cells against the excessive release of redox-active metal ions by scavenging increased mitochondrial superoxide. Neither could our current data exclude the possibility that CDK4-mediated mitochondrial homeostasis is linked with DNA repair capacity. However, increased DNA repair capacity has been reported in LDIR-induced radioadaptive resistance [47,48]. Also the MnSOD activation detoxifies the superoxide that otherwise could generate additional DNA damage. On the other hand, the enhanced mitochondrial respiration may provide additional ATP required for repair of DNA and other large molecules in cells. These results support a cooperative mechanism between the DNA repair system and mitochondrial bioenergetics, which is activated to meet the increased cellular energy demand for quick DNA repair. Identification of the CDK4-mediated mitochondrial homeostasis will help in the development of effective targets for radioprotection of normal cells and radiosensitized tumor cells.

Increasing evidence shows that cell cycle regulators are implicated in the regulation of mitochondrial function and cellular energy metabolism either dependent on or independent of cell cycle progression under normal and stress conditions. CDK4 is the first cell cycle regulator implicated in the control of energy and glucose homeostasis through the regulation of genes participating in glucose metabolism via the CDK4/pRB/E2F pathway [34]. Cyclin D1 represses mitochondrial metabolism through regulation of mitochondrial gene expression, leading to reduced mitochondrial activity and a metabolism shift to glycolysis in vivo [23], whereas CDK4-mediated pRB phosphorylation releases E2F to bind to the promoter region of target genes implicated in metabolism, leading to a switch of energy metabolism from glycolysis to mitochondrial oxidative phosphorylation under the stress of cold and fasting [49]. Nuclear-localized cyclin D1/CDK4 has been found be able to control

glucose homeostasis in postmitotic cells through regulation of gluconeogenic genes independent of cell cycle progression [50]. Under normal physiological conditions, cyclin D1 negatively regulates aerobic glycolysis and mitochondrial size and activity by inducing the expression of a subset of genes governing mitochondrial activity [24], whereas under low-dose radiation stress, cytoplasmic retained cyclin D1 is required for enhanced mitochondrial-mediated antiapoptosis function, leading to adaptive radioprotection [21]. In addition to cyclin D1/CDK4, our previous studies have shown that cyclin B1/CDK1 also participates in the regulation of mitochondrial metabolism either under normal conditions or under low-dose irradiation-induced cellular adaptive response. Under normal conditions, cyclin B1/CDK1 kinase activity is involved in the regulation of mitochondrial metabolism through phosphorylation of mitochondrial electron transport chain complex I subunits in mitochondria, providing energy to cells for the G2/M transition [36], whereas in LDIR-induced cellular adaptive response, mitochondrial-localized cyclin B1/CDK1 can phosphorylate multiple mitochondrial targets, such as p53 and MnSOD [8,51]. Also, our unpublished data indicate that mitochondrial-localized cyclin B1/CDK1 contributes to regulation of SIRT3 enzyme activity through phosphorylation. Our current data extend these findings and demonstrate, for the first time, a new cyclin D1/CDK4/MnSOD network, which communicates with cell cycle kinases and mitochondrial homeostasis via phosphorylation of key mitochondrial factors in LDIR-induced cellular adaptive protection. These results support the concept that an overall status of cell cycle kinase-mediated phosphorylation of mitochondrial targets, such as MnSOD, p53, SIRT3, and complex I subunits, plays a pivotal role in the regulation of mitochondrial homeostasis in cell adaptive response and survival of low levels of genotoxic stress. In addition to cyclin B1/CDK1 and cyclin D1/CDK4 complexes, there might be other currently unknown cell cycle-dependent kinases that are also able to localize to mitochondria and phosphorylate mitochondrial targets to enhance mitochondrial homeostasis under various genotoxic stress conditions, especially sublethal levels of radiation, to allow cells to quickly respond to oxidative stress to adapt and survive. Further elucidation of such a cluster of kinases that control the mitochondrial respiration and antioxidant capacity under different genotoxic conditions may reveal additional new information on the mechanism underlying mitochondrial homeostasis during cell survival. Because CDK4 is activated in the G1/S transition, whereas CDK1 is required for the G2/M transition, it is highly possible that cyclin D1/CDK4-mediated MnSOD phosphorylation and mitochondrial activation are related to mitochondrial regulation under different cellular energy demands during cell cycle progression using the same phosphorylation site of MnSOD.

In summary, this study demonstrates a unique CDK4/MnSOD activation pathway in mitochondrial homeostasis (Fig. 7F), in which mitochondrial-localized cyclin D1/CDK4 phosphorylates MnSOD at serine-106 to quickly increase MnSOD enzymatic activity required for redox balancing and boosted mitochondrial respiration in the cellular adaptive response to environmental genotoxic stress conditions such as low-dose ionizing radiation.

Author Contributions

C.J. and L.Q. performed most of the experiments; Y.S., D.C., C.L., and M.F. conducted the experiments on mitochondrial function; C.J., L.Q., R.L., and M.F. performed the in vivo mouse experiments; R.S. studied the pathological sections of mouse tissues; A.T.V., L.S.W., R.F.L., J.S.M., G.W., D.J.G., and J.J.L. discussed the data and edited the paper; C.J., L.Q., and J.J.L. designed the study and wrote the paper.

Acknowledgments

We appreciate the active discussions with graduate students at Jian Jian Li's lab and the Comparative Pathology Program of the University of California at Davis. This work was supported by the National Institutes of Health (CA152313 to J.J.L.) and the Department of Energy Office of Science (DE-SC0001271 to G.W., J.J.L., D.J.G.).

Appendix A. Supplementary Information

Supplementary data associated with this article can be found the online version at http://dx.doi.org/10.1016/j.freeradbiomed.2014.12.026.

References

[1] Feinendegen, L. E.; Bond, V. P.; Sondhaus, C. A.; Muehlensiepen, H. Radiation effects induced by low doses in complex tissue and their relation to cellular adaptive responses. *Mutat. Res.* **358:**199–205; 1996.
[2] Wolff, S. Are radiation-induced effects hormetic? *Science* **245(575):**621; 1989.
[3] Feinendegen, L. E.; Bond, V. P.; Sondhaus, C. A.; Altman, K. I. Cellular signal adaptation with damage control at low doses versus the predominance of DNA damage at high doses. *C. R. Acad. Sci. III* **322:**245–251; 1999.
[4] Liu, S. Z. Biological effects of low level exposures to ionizing radiation: theory and practice. *Hum. Exp. Toxicol.* **29:**275–281; 2010.
[5] Oberley, L. W.; Buettner, G. R. Role of superoxide dismutase in cancer: a review. *Cancer Res.* **39:**1141–1149; 1979.
[6] McCord, J. M.; Keele Jr. B. B.; Fridovich, I. An enzyme-based theory of obligate anaerobiosis: the physiological function of superoxide dismutase. *Proc. Natl. Acad. Sci. USA* **68:**1024–1027; 1971.
[7] Fan, M.; Ahmed, K. M.; Coleman, M. C.; Spitz, D. R.; Li, J. J. Nuclear factor-kappaB and manganese superoxide dismutase mediate adaptive radioresistance in low-dose irradiated mouse skin epithelial cells. *Cancer Res.* **67:**3220–3228; 2007.
[8] Candas, D.; Fan, M.; Nantajit, D.; Vaughan, A. T.; Murley, J. S.; Woloschak, G. E.; Grdina, D. J.; Li, J. J. CyclinB1/Cdk1 phosphorylates mitochondrial antioxidant MnSOD in cell adaptive response to radiation stress. *J. Mol. Cell Biol.* **5:**166–175; 2013.
[9] Grdina, D. J.; Murley, J. S.; Miller, R. C.; Mauceri, H. J.; Sutton, H. G.; Thirman, M. J.; Li, J. J.; Woloschak, G. E.; Weichselbaum, R. R. A manganese superoxide dismutase (SOD2)-mediated adaptive response. *Radiat. Res.* **179:**115–124; 2013.
[10] Murley, J. S.; Baker, K. L.; Miller, R. C.; Darga, T. E.; Weichselbaum, R. R.; Grdina, D. J. SOD2-mediated adaptive responses induced by low-dose ionizing radiation via TNF signaling and amifostine. *Free Radic. Biol. Med.* **51:**1918–1925; 2011.
[11] Veeraraghavan, J.; Natarajan, M.; Herman, T. S.; Aravindan, N. Low-dose gamma-radiation-induced oxidative stress response in mouse brain and gut: regulation by NFkappaB–MnSOD cross-signaling. *Mutat. Res.* **718:**44–55; 2011.
[12] Yen, H. C.; Oberley, T. D.; Vichitbandha, S.; Ho St Y. S.; Clair, D. K. The protective role of manganese superoxide dismutase against adriamycin-induced acute cardiac toxicity in transgenic mice. *J. Clin. Invest.* **98:**1253–1260; 1996.
[13] Epperly, M. W.; Sikora, C.; Defilippi, S.; Bray, J.; Koe, G.; Liggitt, D.; Luketich, J. D.; Greenberger, J. S. Plasmid/liposome transfer of the human manganese superoxide dismutase transgene prevents ionizing irradiation-induced apoptosis in human esophagus organ explant culture. *Int. J. Cancer* **90:**128–137; 2000.
[14] Niu, Y.; Wang, H.; Wiktor-Brown, D.; Rugo, R.; Shen, H.; Huq, M. S.; Engelward, B.; Epperly, M.; Greenberger, J. S. Irradiated esophageal cells are protected from radiation-induced recombination by MnSOD gene therapy. *Radiat. Res.* **173:**453–-461; 2010.
[15] Murley, J. S.; Kataoka, Y.; Weydert, C. J.; Oberley, L. W.; Grdina, D. J. Delayed radioprotection by nuclear transcription factor kappaB-mediated induction of manganese superoxide dismutase in human microvascular endothelial cells after exposure to the free radical scavenger WR1065. *Free Radic. Biol. Med.* **40:**1004–1016; 2006.
[16] Borgstahl, G. E.; Parge, H. E.; Hickey, M. J.; Beyer Jr. W. F.; Hallewell, R. A.; Tainer, J. A. The structure of human mitochondrial manganese superoxide dismutase reveals a novel tetrameric interface of two 4-helix bundles. *Cell* **71:**107–118; 1992.
[17] Chen, Y.; Zhang, J.; Lin, Y.; Lei, Q.; Guan, K. L.; Zhao, S.; Xiong, Y. Tumour suppressor SIRT3 deacetylates and activates manganese superoxide dismutase to scavenge ROS. *EMBO Rep.* **12:**534–541; 2011.
[18] Tao, R.; Coleman, M. C.; Pennington, J. D.; Ozden, O.; Park, S. H.; Jiang, H.; Kim, H. S.; Flynn, C. R.; Hill, S.; Hayes McDonald, W.; Olivier, A. K.; Spitz, D. R.; Gius, D. Sirt3-mediated deacetylation of evolutionarily conserved lysine 122 regulates MnSOD activity in response to stress. *Mol. Cell* **40:**893–904; 2010.
[19] Quijano, C.; Hernandez-Saavedra, D.; Castro, L.; McCord, J. M.; Freeman, B. A.; Radi, R. Reaction of peroxynitrite with Mn-superoxide dismutase: role of the metal center in decomposition kinetics and nitration. *J. Biol. Chem.* **276:**11631–11638; 2001.

[20] Roue, G.; Pichereau, V.; Lincet, H.; Colomer, D.; Sola, B. Cyclin D1 mediates resistance to apoptosis through upregulation of molecular chaperones and consequent redistribution of cell death regulators. *Oncogene* **27:**4909–4920; 2008.
[21] Ahmed, K. M.; Fan, M.; Nantajit, D.; Cao, N.; Li, J. J. Cyclin D1 in low-dose radiation-induced adaptive resistance. *Oncogene* **27:**6738–6748; 2008.
[22] Agami, R.; Bernards, R. Distinct initiation and maintenance mechanisms cooperate to induce G1 cell cycle arrest in response to DNA damage. *Cell* **102:**55–66; 2000.
[23] Sakamaki, T.; Casimiro, M. C.; Ju, X.; Quong, A. A.; Katiyar, S.; Liu, M.; Jiao, X.; Li, A.; Zhang, X.; Lu, Y.; Wang, C.; Byers, S.; Nicholson, R.; Link, T.; Shemluck, M.; Yang, J.; Fricke, S. T.; Novikoff, P. M.; Papanikolaou, A.; Arnold, A.; Albanese, C.; Pestell, R. Cyclin D1 determines mitochondrial function in vivo. *Mol. Cell. Biol.* **26:**5449–5469; 2006.
[24] Wang, C.; Li, Z.; Lu, Y.; Du, R.; Katiyar, S.; Yang, J.; Fu, M.; Leader, J. E.; Quong, A.; Novikoff, P. M.; Pestell, R. G. Cyclin D1 repression of nuclear respiratory factor 1 integrates nuclear DNA synthesis and mitochondrial function. *Proc. Natl. Acad. Sci. USA* **103:**11567–11572; 2006.
[25] Sumrejkanchanakij, P.; Tamamori-Adachi, M.; Matsunaga, Y.; Eto, K.; Ikeda, M. A. Role of cyclin D1 cytoplasmic sequestration in the survival of postmitotic neurons. *Oncogene* **22:**8723–8730; 2003.
[26] Hagen, K. R.; Zeng, X.; Lee, M. Y.; Tucker Kahn, S.; Harrison Pitner, M. K.; Zaky, S. S.; Liu, Y.; O'Regan, R. M.; Deng, X.; Saavedra, H. I. Silencing CDK4 radiosensitizes breast cancer cells by promoting apoptosis. *Cell Div* **8:**10; 2013.
[27] Spitz, D. R.; Oberley, L. W. An assay for superoxide dismutase activity in mammalian tissue homogenates. *Anal. Biochem.* **179:**8–18; 1989.
[28] Frezza, C.; Cipolat, S.; Scorrano, L. Organelle isolation: functional mitochondria from mouse liver, muscle and cultured fibroblasts. *Nat. Protoc.* **2:**287–295; 2007.
[29] Lu, G.; Ren, S.; Korge, P.; Choi, J.; Dong, Y.; Weiss, J.; Koehler, C.; Chen, J. N.; Wang, Y. A novel mitochondrial matrix serine/threonine protein phosphatase regulates the mitochondria permeability transition pore and is essential for cellular survival and development. *Genes Dev.* **21:**784–796; 2007.
[30] Mukhopadhyay, P.; Rajesh, M.; Hasko, G.; Hawkins, B. J.; Madesh, M.; Pacher, P. Simultaneous detection of apoptosis and mitochondrial superoxide production in live cells by flow cytometry and confocal microscopy. *Nat. Protoc.* **2:**2295–2301; 2007.
[31] Vives-Bauza, C.; Yang, L.; Manfredi, G. Assay of mitochondrial ATP synthesis in animal cells and tissues. *Methods Cell Biol.* **80:**155–171; 2007.
[32] Marchal, J. A.; Nunez, M. C.; Suarez, I.; Diaz-Gavilan, M.; Gomez-Vidal, J. A.; Boulaiz, H.; Rodriguez-Serrano, F.; Gallo, M. A.; Espinosa, A.; Aranega, A.; Campos, J. M. A synthetic uracil derivative with antitumor activity through decreasing cyclin D1 and Cdk1, and increasing p21 and p27 in MCF-7 cells. *Breast Cancer Res. Treat.* **105:**237–246; 2007.
[33] Malumbres, M.; Barbacid, M. To cycle or not to cycle: a critical decision in cancer. *Nat. Rev. Cancer* **1:**222–231; 2001.
[34] Blanchet, E.; Annicotte, J. S.; Fajas, L. Cell cycle regulators in the control of metabolism. *Cell Cycle* **8:**4029–4031; 2009.
[35] Tamamori-Adachi, M.; Ito, H.; Sumrejkanchanakij, P.; Adachi, S.; Hiroe, M.; Shimizu, M.; Kawauchi, J.; Sunamori, M.; Marumo, F.; Kitajima, S.; Ikeda, M. A. Critical role of cyclin D1 nuclear import in cardiomyocyte proliferation. *Circ. Res.* **92:**e12–e19; 2003.
[36] Wang, Z.; Fan, M.; Candas, D.; Zhang, T. Q.; Qin, L.; Eldridge, A.; Wachsmann-Hogiu, S.; Ahmed, K. M.; Chromy, B. A.; Nantajit, D.; Duru, N.; He, F.; Chen, M.; Finkel, T.; Weinstein, L. S.; Li, J. J. Cyclin B1/Cdk1 coordinates mitochondrial respiration for cell-cycle G2/M progression. *Dev. Cell* **29:**217–232; 2014.
[37] Henderson, J. R.; Swalwell, H.; Boulton, S.; Manning, P.; McNeil, C. J.; Birch-Machin, M. A. Direct, real-time monitoring of superoxide generation in isolated mitochondria. *Free Radic. Res.* **43:**796–802; 2009.
[38] Rigoulet, M.; Yoboue, E. D.; Devin, A.; Mitochondrial, ROS generation and its regulation: mechanisms involved in H_2O_2 signaling. *Antioxid. Redox Signaling* **14:**459–468; 2011.
[39] Figueira, T. R.; Barros, M. H.; Camargo, A. A.; Castilho, R. F.; Ferreira, J. C.; Kowaltowski, A. J.; Sluse, F. E.; Souza-Pinto, N. C.; Vercesi, A. E. Mitochondria as a source of reactive oxygen and nitrogen species: from molecular mechanisms to human health. *Antioxid. Redox Signaling* **18:**2029–2074; 2013.
[40] Balaban, R. S.; Nemoto, S.; Finkel, T. Mitochondria, oxidants, and aging. *Cell* **120:**483–495; 2005.
[41] Dhar St S. K.; Clair, D. K. Manganese superoxide dismutase regulation and cancer. *Free Radic. Biol. Med.* **52:**2209–2222; 2012.
[42] Stohs, S. J.; Bagchi, D. Oxidative mechanisms in the toxicity of metal ions. *Free Radic. Biol. Med.* **18:**321–336; 1995.
[43] Leonard, S. S.; Harris, G. K.; Shi, X. Metal-induced oxidative stress and signal transduction. *Free Radic. Biol. Med.* **37:**1921–1942; 2004.
[44] Valko, M.; Rhodes, C. J.; Moncol, J.; Izakovic, M.; Mazur, M. Free radicals, metals and antioxidants in oxidative stress-induced cancer. *Chem. Biol. Interact.* **160:**1–40; 2006.
[45] Lee, J. C.; Son, Y. O.; Pratheeshkumar, P.; Shi, X. Oxidative stress and metal carcinogenesis. *Free Radic. Biol. Med.* **53:**742–757; 2012.
[46] Hureaua, C. Coordination of redox active metal ions to the amyloid precursor protein and to amyloid-β peptides involved in Alzheimer disease. *Coord. Chem. Rev.* **256:**2164–2174; 2012.
[47] Pollycove, M. Radiobiological basis of low-dose irradiation in prevention and therapy of cancer. *Dose Response* **5:**26–38; 2007.
[48] Phan, N.; De Lisio, M.; Parise, G.; Boreham, D. R. Biological effects and adaptive response from single and repeated computed tomography scans in reticulocytes and bone marrow of C57BL/6 mice. *Radiat. Res.* **177:**164–175; 2012.
[49] Blanchet, E.; Annicotte, J. S.; Lagarrigue, S.; Aguilar, V.; Clape, C.; Chavey, C.; Fritz, V.; Casas, F.; Apparailly, F.; Auwerx, J.; Fajas, L. E2F transcription factor-1 regulates oxidative metabolism. *Nat. Cell Biol.* **13:**1146–1152; 2011.
[50] Lee, Y.; Dominy, J. E.; Choi, Y. J.; Jurczak, M.; Tolliday, N.; Camporez, J. P.; Chim, H.; Lim, J. H.; Ruan, H. B.; Yang, X.; Vazquez, F.; Sicinski, P.; Shulman, G. I.; Puigserver, P. Cyclin D1–Cdk4 controls glucose metabolism independently of cell cycle progression. *Nature* **510:**547–551; 2014.
[51] Nantajit, D.; Fan, M.; Duru, N.; Wen, Y.; Reed, J. C.; Li, J. J. Cyclin B1/Cdk1 phosphorylation of mitochondrial p53 induces anti-apoptotic response. *PLoS One* **5:**e12341; 2010.